Origin of Retinal Pigment Epithelium Cell Damage by Pulsed Laser Irradiance in the Nanosecond to Microsecond Time Regimen

Ralf Brinkmann, MSc,[1]* Gereon Hüttmann, PhD,[1] Jan Rögener, MSc,[1] Johann Roider, MD,[2] Reginald Birngruber, PhD,[1] and Charles P. Lin, PhD[3]

[1]*Medical Laser Center Lübeck GmbH, Lübeck, Germany*
[2]*University of Regensburg, Eye Clinic, Regensburg, Germany*
[3]*Wellman Laboratories of Photomedicine, Massachusetts General Hospital, Harvard Medical School, Boston, Massachusetts*

Background and Objective: Selective photodamage of the retinal pigment epithelium (RPE) is a new technique to treat a variety of retinal diseases without causing adverse effects to surrounding tissues such as the neural retina including the photoreceptors and the choroid. In this study, the mechanism of cell damage after laser irradiation was investigated.
Study Design/Materials and Methods: Single porcine RPE-melanosomes and RPE cells were irradiated with a Nd:YLF laser (wavelength $\lambda = 527$ nm, adjustable pulse duration $\tau = 250$ nsec-3 μsec) and a Nd:YAG laser ($\lambda = 532$ nm, $\tau = 8$ nsec). Fast flash photography was applied to observe vaporization at melanosomes in suspension. A fluorescence viability assay was used to probe the cells vitality.
Results: The threshold radiant exposures for vaporization around individual melanosomes and for ED_{50} cell damage are similar at 8-nsec pulse duration. Both thresholds increase with pulse duration; however, the ED_{50} cell damage radiant exposure is 40% lower at 3μsec. Temperature calculations to model the onset of vaporization around the melanosomes are in good agreement with the experimental results when assuming a surface temperature of 150°C to initiate vaporization and a homogeneous melanosome absorption coefficient of 8,000 cm^{-1}. Increasing the number of pulses delivered to RPE cells at a repetition rate of 500 Hz, the ED_{50} value decreases for all pulse durations. However, the behavior does not obey scaling laws such as the $N^{1/4}$ equation.
Conclusion: The origin of RPE cell damage for single pulse irradiation up to pulse durations of 3 μsec can be described by a damage mechanism in which microbubbles around the melanosomes cause a rupture of the cell structure. The threshold radiant exposure for RPE damage decreases with increasing number of pulses applied. Lasers Surg. Med. 27:451–464, 2000.   © 2000 Wiley-Liss, Inc.

Key words: fast flash photography; fluorescence microscopy; melanosome; pulse stretched laser; RPE-damage; selective photocoagulation; viability assay

INTRODUCTION

A variety of retinal diseases such as diabetic macular edema, drusen, and central serous retinopathy are thought to be associated with a decreased function of retinal pigment epithelial cells (RPE cells). A method for selective destruction of these cells without causing adverse effects to adjacent tissue, especially to the neural retina, the

photoreceptors and the choroid, seems to be an appropriate method of treatment [1], presuming that the damaged cells will be replaced by proliferation or migration of neighboring intact RPE cells.

The selective damage of the RPE has first been demonstrated by Roider et al. in rabbits by using 5-μsec Argon-ion laser pulses at 514 nm at a repetition rate of 500 Hz [2]. Fluorescein angiography was applied to visualize the ophthalmoscopically invisible effects. The selectivity of the damage to RPE cells, sparing the photoreceptors was demonstrated by histologic examinations at different times after treatment. Two weeks after laser exposure, the lesions were covered by a new population of RPE cells. Four weeks after treatment, a morphologically completely restored RPE barrier showing normal RPE cells was found [2].

A first clinical trial has already proved the concept of selective RPE destruction with a train of microsecond laser pulses and demonstrated the clinical potential of this technique [3,4]. Microperimetry, as tested with the threshold stimulus, showed no loss of retinal function in the follow-up period of one year and demonstrated the selectivity of this technique[5,6].

For visible light, the main chromophores in the fundus are melanosomes inside the RPE cells (Fig. 1) [7], which absorb approximately 50% of the incident light [8]. When the fundus is irradiated with laser pulses at a pulse duration below 5 μsec, high temperatures are mainly confined to the RPE cells and only a low sublethal temperature increase in the adjacent tissue structures is obtained [1].

According to the model of Arrhenius [9], the rate of thermal damage to tissue increases strongly with temperature. By using single pulses of few microseconds in duration, significant thermal damage is only caused in the regions of very high temperatures, which may lead to photodisruptive effects such as choroidal bleeding. To avoid high peak temperatures, multiple pulses were used in preclinical and clinical studies to reduce the peak temperatures by using the additivity of thermal effects. The mechanism of the selective photocoagulation, therefore, was thought to be thermal necrosis of the cell.

Apart from a primary thermal effect as postulated by Roider et al. [1], thermomechanical damage of the cells has to be taken into account: Lin and Kelly heated microabsorbers in suspension with picosecond and nanosecond laser pulses and demonstrated vaporization around the par-
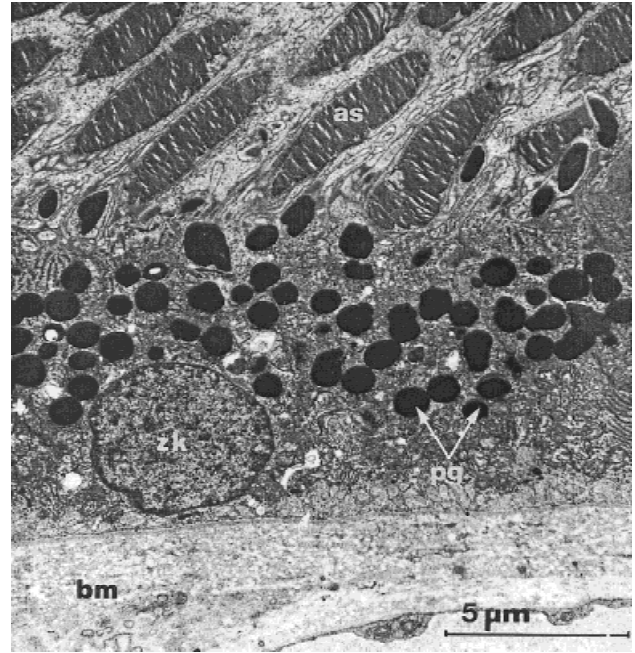

Fig. 1. Transmission electron microscopy (TEM) of a normal human pigment epithelium [7]. bm, Bruch's membrane; zk, cell nucleus; pg, melanosomes; as, outer side of photoreceptors.

ticles [10]. A threshold radiant exposure for microbubble formation around bovine melanosomes was found to be 55 mJ/cm^2 at a wavelength of 532 nm. Irradiating RPE cells at the same radiant exposure, nonviable cells were only found, when intracellular bubble formation occurred [11]. It was concluded that cell death is caused by thermomechanical disruption of the cell structure due to the significantly increased cell volume during bubble life time.

RPE cell damage caused by stress waves was investigated in vitro by Douki et al. They found that cell damage is rather dependent on the stress rise time as on the peak stress and requires stress transients around 70 bar/nsec [12]. In selective RPE photocoagulation in vivo, Roider et al. also postulated a mechanical effect to cause RPE cell damage when repetitively applying a train of 200-nsec pulses to rabbit eyes [13]. An excellent review article summarizing laser-induced thermal damage mechanisms in the retina and discussing different melanin granule models is given by Thompson et al. [14].

The objective of this study was to investigate whether a thermomechanical mechanism might be responsible for selective RPE cell damage when laser pulse durations up to several microseconds are used. Therefore, the vaporization threshold radiant exposure around single melano-

somes and the ED_{50} threshold to cause RPE-cell damage after laser irradiation was investigated by fast flash photography and a cell viability assay, respectively. To investigate the range of pulse durations between nanoseconds and microseconds, two laser systems were used: A Q-switched, pulse-stretched Nd:YLF laser with adjustable pulse duration between 250 nsec and 3 μsec at a wavelength of 527 nm and a Q-switched, frequency doubled Nd:YAG laser at a wavelength of 532 nm and 8-nsec exposure time. As a model system, porcine and bovine melanosomes in suspension and porcine RPE cell layers were used. The melanosomes were irradiated with single pulses to probe vaporization while the RPE-cells were irradiated with single and multiple pulses at a repetition rate of 500 Hz. To analyze the results, temperature increase during and after irradiation in the surroundings of melanosomes was calculated. Cell damage as an effect of bubble formation in this pulse regimen is discussed extensively and is analyzed with respect to a pure thermally and a stress wave-induced damage.

MATERIALS AND METHODS
Laser Systems

An arc-lamp excited, intracavity frequency doubled Nd:YLF laser (Quantronix, Inc., model 527DP-H) was modified with an active feedback electro-optical Q-switched system to generate pulse durations up to several microseconds at a wavelength of 527 nm. Operating the system in the normal Q-switched mode, the laser emits pulses of typically 250 nsec in duration with pulse energies of several millijoules at a repetition rate of 500 Hz. To extend the pulse duration, a transient high voltage course was applied to the Pockel's-cell to increase cavity losses during pulse emission. A more detailed description of the configuration used for pulse-stretching can be find elsewhere [15]. The energy was transmitted by a 105-μm core diameter fiber (Ceram Optec GmbH, Optran UV-A 105/125/250, NA = 0.22). The length of the fiber was 200 m to minimize spatial and temporal intensity modulation at the distal fiber tip. Pulse durations of 8 nsec were generated with a flashlamp pumped Q-switched and frequency doubled Nd:YAG laser (Spectron Inc.) at a wavelength of 532 nm. An experiment to probe the threshold for bubble formation on bovine melanosomes was performed with a Nd:YAG laser which emits pulse durations of 20 nsec at a wavelength of 532 nm (SEO 123 - Nd:YAG).

Experimental Setup

The experimental setup to irradiate the samples, either melanosomes in suspension or complete RPE cell layers, is shown in Figure 2. By imaging the distal fiber tip to the object plane, a circular spot of 47 μm diameter was irradiated. The deviation of the radiant exposure from a constant top hat beam profile was below 10% across the spot. The suspension of melanosomes was collinearly illuminated with a N_2-pumped dye laser (Laser Science, Inc., VSL-337ND) (670 nm, 1 nsec) to probe vaporization occurring around the melanosomes during irradiation. A variable electronic delay was used to trigger the N_2 laser with the Nd:YLF or Nd:YAG laser, allowing to shift the probe pulse relative to the irradiation laser pulse. The images were recorded with a standard CCD-camera and a frame grabber. A photo diode (EG&G, FND 100) with a current integrating circuit, which was calibrated against a pyroelectric energy meter (DigiRad R-752 / P-444), was used to determine the pulse energy.

Porcine Eye Model, Viability Assay, and Threshold Irradiances

RPE tissue samples and melanosomes were harvested from freshly enucleated porcine eyes. Figure 3 shows a TEM picture, cut parallel to the porcine RPE cell layer. RPE cell samples were prepared by taking circular section of 1 cm^2 from the fundus of the eye including retina, sclera, and choroid. The neural retina was carefully pealed off. Marker lesions that used pulse energies far above damage threshold were placed on the samples. In several rows and columns, the sample was irradiated between the marker lesions with the different exposure parameters. RPE cell vitality was probed by the fluorescent dye marker Calcein-AM (Molecular Probes, Inc.), which tags living cells. In living cells, Calcein-AM is transformed to Calcein by esterases. Calcein can be excited with blue light (excitation maximum at 490 nm) to fluoresce in the green spectral region. Calcein-AM was used in a phosphate buffer solution at a concentration of 2μg/ml. Twenty milliliters were dropped onto the RPE cell layer directly after irradiation. The sample was covered with a microscope cover slide to prevent desiccation. The nonfluorescing cells were counted under a fluorescence microscope 30 minutes after irradiation.

For all parameter sets, samples from 10 different eyes have been used, except for the experiment with the 3-μsec, 50 pulses, the data were derived from four different eyes only. Several
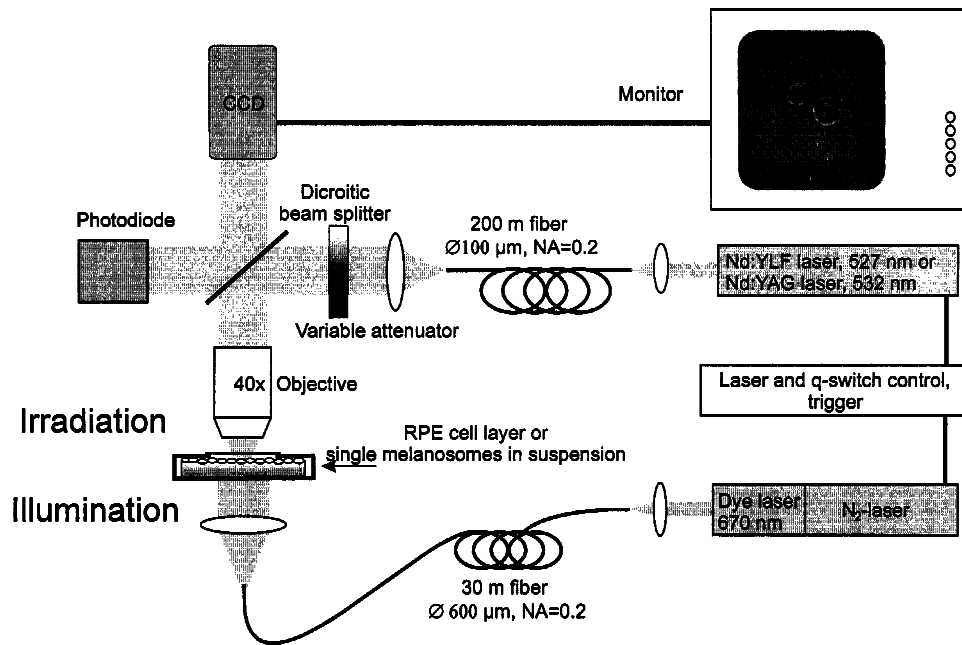
Fig. 2. Experimental setup to irradiate melanosomes in suspension and RPE-cell samples with the Nd:YLF or Nd:YAG laser. The N_2-pumped dye laser is used to probe vaporization around melanosomes in suspension. A typical photograph of microbubbles is shown on the monitor, the radiant exposure was two times above threshold.

spots of approximately 10 RPE cells were irradiated at three to six different energy levels. A total of approximately 1,000 cells per data point has been used to calculate the ED_{50} and the fiducial limits at 95% confidence levels by using the probit analysis [16].

Bubble Formation Thresholds at Single Melanosomes

Melanosomes were extracted from RPE cells and suspended in distilled water. Several drops were placed on standard microscope slides, covered with cover slips, which were sealed to prevent evaporation of water. The vaporization threshold radiant exposure on single melanosomes was determined by varying the pulse energy with a variable attenuator (Fig. 2) and the probe flash delay relative to the laser pulse until minimal visible bubbles of approximately 2 μm in diameter occurred. The reported threshold radiant exposures are the mean of 10 melanosomes per eye from six different eyes. The error bar indicates the standard deviation between the mean values of each eye.

To further elucidate the mechanism of bubble formation, particle suspensions of melanosomes were preequilibrated at various temperatures T_{eq} between 25 and 80°C, and the threshold
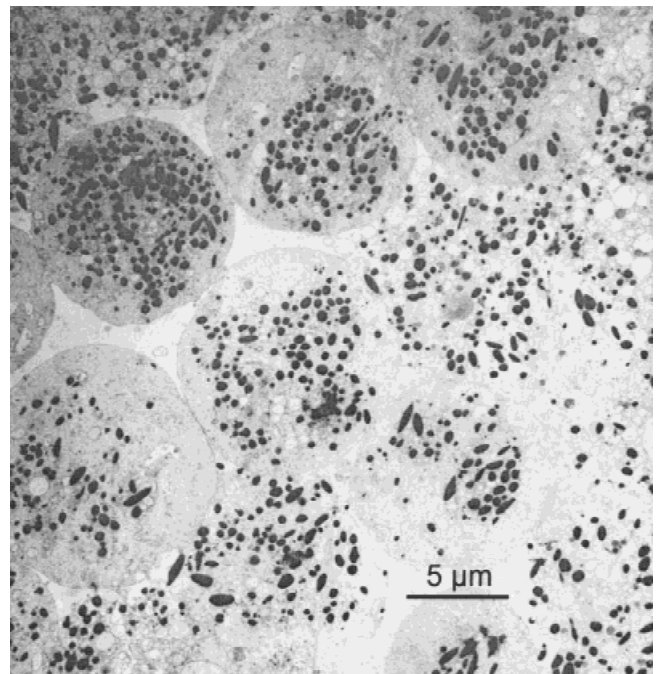

Fig. 3. Transmission electron microscopy (TEM) of a porcine retinal pigment epithelium (RPE) cell layer. The cell layer is cut nearly parallel to Bruch's membrane. The left upper corner shows the melanosome distribution in the upper parts of a cell, whereas the deeper lying nucleus in the lower cell part is shown in the right bottom corner.

radiant exposure F_{th} for bubble formation was determined for each T_{eq} by using the time-resolved imaging technique. The threshold temperature for bubble formation T_{th} is related to the radiant exposure F_{th} by the equation.

$$T_{th} - T_{eq} = \frac{\mu_a}{c_p \cdot \rho} \cdot F_{th}$$

where μ_a is the absorption coefficient, ρ the density, and c_p the specific heat of the particles.

Temperature Calculations

Temperature distributions in and around the melanosomes were calculated by using an analytical solution of the equation for heat diffusion for a spherical particle [17]. This model was described in detail by Thompson et al. [14]. In short, single melanosomes are modeled by spheres with a diameter of 1 μm, having the thermal properties of water. For the surrounding tissue, the heat capacity and the diffusivity of water were used as well. Inside the sphere, heat is produced spatially homogeneously throughout the volume at constant rate during the laser pulse. The optical energy, which is absorbed by a melanosome during irradiation, was calculated by assuming a homogeneously absorbing macroscopic sphere with a certain absorption coefficient [18]. Corrections for the higher index of refraction of melanin and coherent effects due to the small size of the particles were not made. The threshold for bubble formation was calculated for different pulse durations from the radiant exposure, which is needed to generate a certain threshold temperature at the surface of a melanosome.

Temperature distributions inside the RPE layer were calculated by superposition of the temperature distributions of a large number of individual melanosomes, which were placed on a regular rectangular grid in a cylindrical volume. The linearity of the heat diffusion equation justifies this simple approach for calculating temperature in a medium, which is homogeneous except for its absorption. To speed up the calculation time, the temperature distribution of more distant melanosomes was calculated from the temperature at a thermal point source. Screening of deeper lying melanosomes to the incoming irradiation was not taken into account.

For a calculation of the average RPE-temperature, which builds up during the irradiation with multiple pulses, a simple thermal model can be used. During the 2 msec, which separates the pulses, the temperature is equalized by heat diffusion over a distance of approximately 100 μm. In this case, the granular structure of the absorbing melanosomes can be neglected and the thickness of the RPE does not influence the background temperature. Therefore, the irradiated area was modeled by a homogeneously absorbing disk with a thickness of 5 μm corresponding to the thickness of the melanosome layer, and a diameter of 50 μm. The temperature in the center of this disk was calculated for pulsed and continuous irradiation by an analytical solution of the heat diffusion equation [19]. The absorption in the choroid was neglected. All calculations were performed on PC by using Mathematica 3.0.

RESULTS

Pulse Stretched Nd:YLF Laser

Typical pulse shapes achieved with the Nd:YLF laser system are shown in Figure 4 by using constant pump conditions at a pulse repetition rate of 500 Hz. In the normal Q-switched operation, pulse durations of typically 250-nsec full width at half maximum (FWHM) are emitted. Extending the laser pulses at constant pump conditions unavoidably leads to a reduced pulse energy because increased cavity losses result in an increased final population inversion density of the laser medium [15,20]. Starting with a pulse energy of 2 mJ at a pulse duration of 250 nsec, typically 60% of the energy is achieved at a pulse duration of 1 μsec, which is further reduced to approximately 25% of the initial value at a pulse duration of 3 μsec.

Temperature Dependence of the Bubble Formation Thresholds at Single Melanosomes

Figure 5 shows the temperature dependence of bubble formation threshold for bovine melanosomes suspended in water, when irradiated with 532 nm, 20-nsec laser pulses. Experimentally measured values of F_{th} plotted against T_{eq} gave a straight regression line. By extrapolating the linear regression to the horizontal axis, a threshold temperature T_{th} of approximately 150°C can be read at the intercept. An absorption coefficient of $\mu_a = 9{,}900$ cm^{-1} can be calculated from the slope of the linear fit by using equation (1).

Near threshold, a bubble can be repeatedly produced around a melanosome after each pulse, without destroying the particle, suggesting that the observed bubble is a "vapor blanket" rather
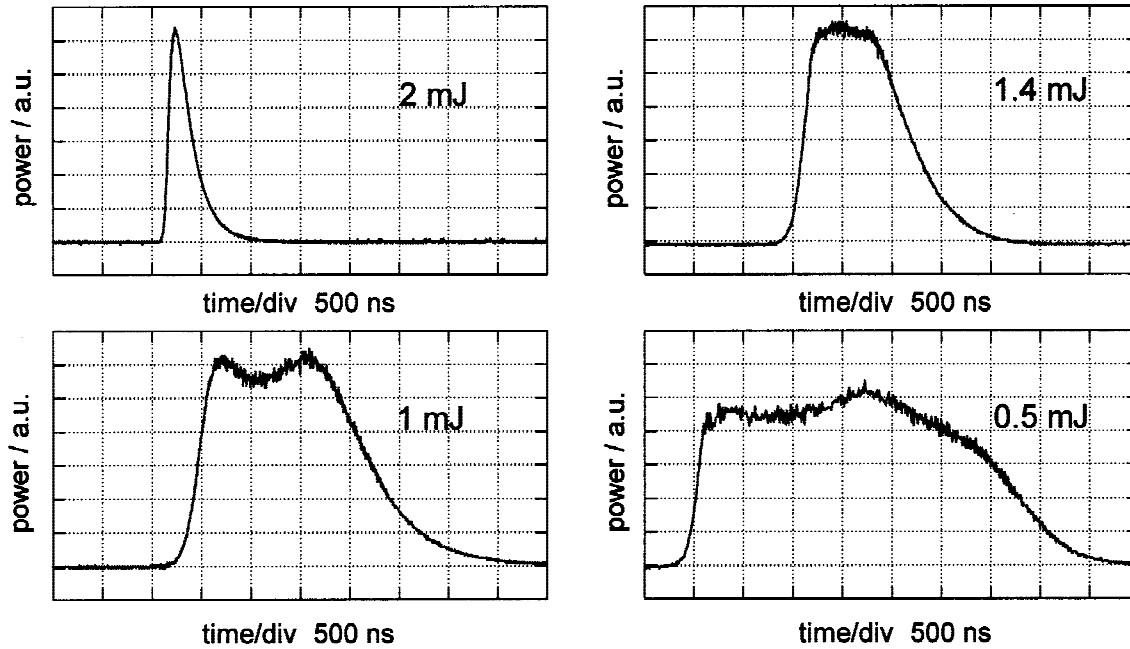
Fig. 4. Typical pulse shapes achieved with the pulse stretched Nd:YLF laser under constant pump conditions at a wavelength of 527 nm and pulse repetition rate of 500 Hz. The plots show pulse durations of 250 nsec, 1.1 μsec, 1.7 μsec, and 3.1 μsec full width at half maximum with the corresponding pulse energies.
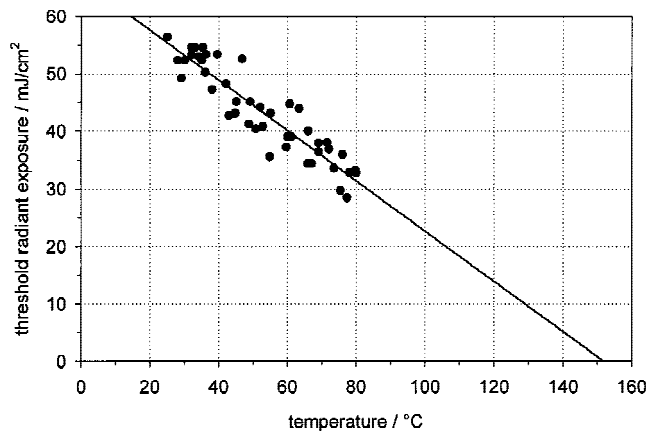

Fig. 5. Temperature dependence of the vaporization threshold for bovine melanosomes suspended in water, after 532-nm 20-nsec pulses.

than a vaporized core. At high radiant exposures (e.g., > 5× threshold), the particles are fragmented after a single or a few laser pulses.

Bubble Formation Thresholds at Single Melanosomes and ED$_{50}$ Damage Threshold of RPE Cells With Single Pulses

Figure 6 depicts the threshold radiant exposures for bubble formation around single melano-

somes and the ED$_{50}$ value of RPE cell damage at different pulse durations when irradiated with one single laser pulse. Applying 8-nsec pulses, the threshold radiant exposure for melanosomes and RPE cells is similar at 90 and 84 mJ/cm^2, respectively. The threshold for bubble formation at single melanosomes increases by nearly a factor of 2 at a pulse duration of 250 nsec and further increases almost linearly with pulse duration up to 552 mJ/cm^2 at 3 μsec. The threshold for RPE cell damage also increases with pulse duration. However, for longer pulses the threshold is significantly lower as the bubble formation threshold at single melanosomes. At a pulse duration of 3 μsec, only 40% of the energy is needed for 50% cell damage.

RPE Damage Threshold for Irradiation With Multiple Pulses

When the RPE is irradiated with a train of pulses at a pulse repetition rate of 500 Hz, a decrease of the threshold radiant exposure for cell damage is observed as shown in Figure 7. With 50% at 10^4 pulses, the decrease is most pronounced at a pulse width of 3 μsec. The threshold is mostly reduced during the first 500 pulses. By
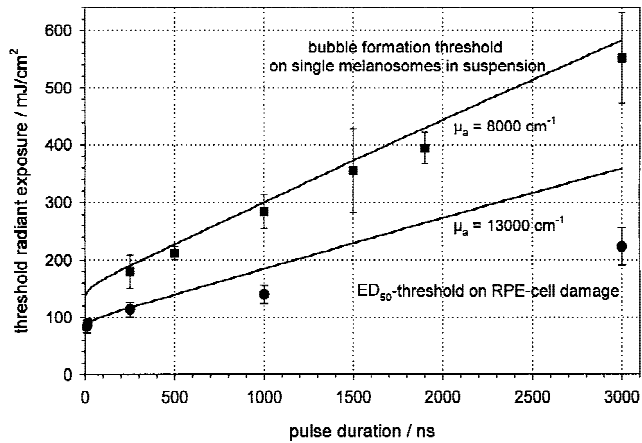
Fig. 6. Threshold radiant exposures as a function of pulse duration for bubble formation around single melanosomes in suspension (squares) and ED_{50} damage of retinal pigment epithelium (RPE) cells (dots). The solid lines represent the calculated threshold radiant exposure assuming vaporization is initiated at a surface temperature of 150°C. Absorption coefficients of 8,000 and 13,000 cm^{-1} were used.
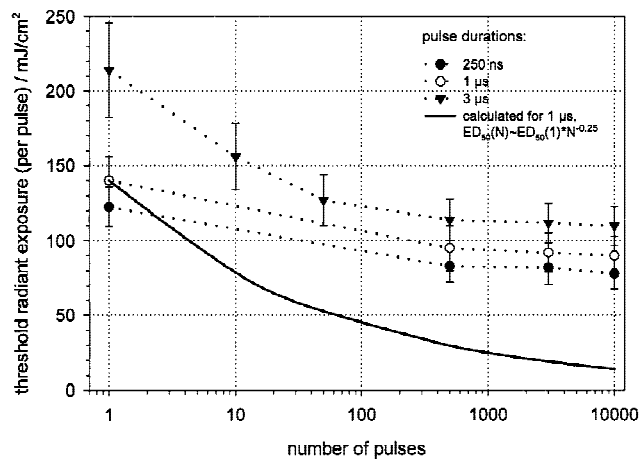

Fig. 7. Threshold of retinal pigment epithelium (RPE) cell damage as a function of the number of pulses applied at a pulse repetition rate of 500 Hz. Pulse durations are 250 nsec, 1 µsec, and 3 µsec. The solid line represents a fit scaling damage according to $ED_{50}(N) = ED_{50}(1) \times N^{1/4}$ (see text for details).

using longer pulse series, the damage threshold does only decrease slightly.

The solid line in Figure 7 shows a fit according to a commonly used empirical law scaling damage of tissue when regarding the accumulative effect of N pulses. According to this relation, $ED_{50}(N) = ED_{50}(1) * N^{1/4}$, the solid line represents the expected threshold decrease, exemplary shown for the pulse duration of 1 µsec. It shows a monotonously decreasing curve starting from the
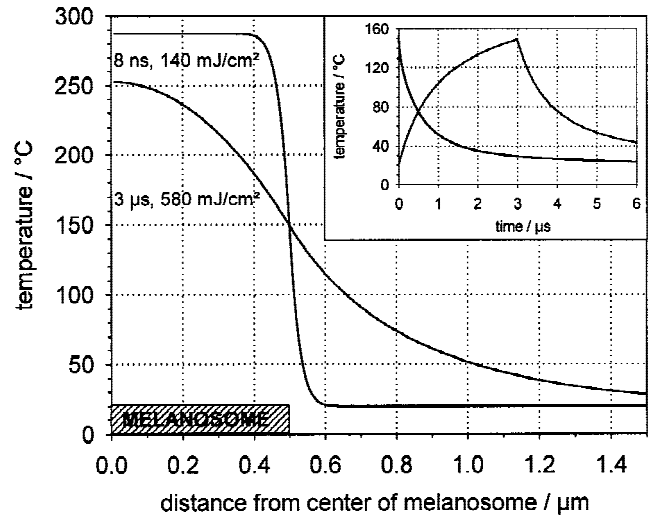

Fig. 8. Temperature course calculated inside and around a spherical melanosome with a diameter of 1 µm at the end of a laser pulse, when using pulse durations of 8 nsec and 3 µsec, respectively. Radiant exposures of 140 and 580 mJ/cm^2 are needed to achieve a surface temperature of 150°C ($\mu_a = 8000$ cm$^{\pm1}$, base temperature: 20°C). The inlay depicts the temperature course at the surface of a melanosome during laser exposure for both cases.

initial value of 140 mJ/cm^2, without showing any saturation at higher number of pulses.

Temperature calculations at single melanosomes, a grid of melanosomes, and the RPE layer

To understand the increase of the bubble formation threshold for longer pulse durations as shown in Figure 6, the threshold radiant exposure to initiate vaporization was calculated: From the extrapolation shown in Figure 5, the threshold temperature for vaporization at the surface of a melanosome was assumed to be 150°C. The absorption coefficient of the melanosomes was fitted to match the measured threshold values for microbubble formation at single particles in Figure 6. In all cases, a homogeneous energy uptake within the melanosome was assumed and an appropriate homogeneous absorption coefficient was used.

The temperature evolution at and around a single melanosome after applying a single laser pulse is shown in Figure 8. With a pulse duration of 8 nsec, the thermal energy is confined to a 1-µm melanosome during the irradiation. At the end of the laser pulse, when the highest temperature on the surface is reached, a nearly rectangular temperature distribution results between particle and the surrounding (Fig. 8). Assuming an ab-

sorption coefficient of 8,000 cm^{-1} with a radiant exposure of 140 J/cm^2, a temperature increase of 130°K is reached at the surface of the melanosomes. With 3-μsec pulse duration, a radiant exposure of 580 mJ/cm^2 is needed to obtain the same surface temperature at the end of the pulse, because a considerable amount of energy diffuses out of the melanosomes and heats the surrounding water during pulse emission. After the end of the irradiation, it takes approximately 5 μsec for the melanosome to cool down (inset of Fig. 8).

Thus, the calculation predict an increase of the threshold radiant exposure for bubble formation at single melanosomes. With a threshold temperature of 150°C and absorption coefficient of 8,000 cm^{-1}, the calculated bubble formation thresholds are in good agreement with the experimental data (Fig. 6) for a pulse duration of 250 nsec and longer. For the 8-nsec pulse, the calculated value is higher by 40%. By using an absorption coefficient of 13,000 cm^{-1}, the threshold radiant exposure for an 8-nsec pulse is matched; however, by using this absorption coefficient for longer pulse durations, the calculated thresholds are below the experimental data.

In the RPE, neighboring melanosomes of different size and shape are separated by random distances, which vary between contact and a few hundred nanometers as shown in Figures 1 and 3. Therefore, individual melanosomes are also heated by their neighbors if the pulse duration is long enough to allow heat flow over these distances. This behavior is principally demonstrated in Figure 9, which shows the temperature increase at the surface of a single central melanosome of 1 μm in diameter, embedded between multiple melanosomes in a cylindrical volume of a height of 10 μm and a diameter of 50 μm. Temperature courses were calculated for a radiant exposure of 100 mJ/cm^2 at four different pulse duration (250 nsec, 1, 3, and 5 μsec) and for different particle distances. In the calculations, the grid of the melanosomes was constructed with a separation of the particle surfaces of 0.25, 0.5, and 1.5 μm. An absorption coefficient of 10^4 cm^{-1} was assumed for a single melanosome. Each temperature curve shows an increase of the temperature during the laser pulse and a cooling within a few microseconds, which leads to an elevated average temperature of the RPE layer. The cooling time for the whole RPE layer is in the order of a few hundred microseconds. The difference of the maximal temperature for nano- and microsecond pulses is lower as the melanosomes are packed
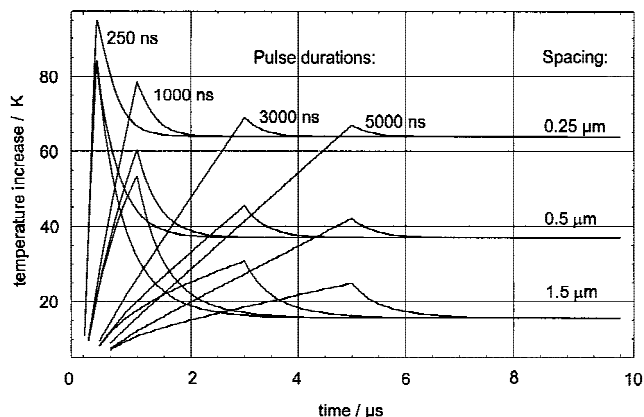

Fig. 9. Temperature at the surface of a melanosome in the center of a cylindrical field of melanosomes. The plots depict the time course of the surface temperature for different pulse durations and spacing between adjacent absorbers in the mash. To resemble the situation, the thickness of the field was 10 μm with a diameter of 50 μm. A radiant exposure of 100 mJ/cm^2 was assumed with an absorption coefficient of 10,000 $cm^{±1}$ per particle.

more densely. For 1.5-μm distance between the surfaces, a 250-nsec pulse generates a peak 3× higher than a 5-μsec pulse, whereas for 0.25-μm separation those temperatures vary only by a factor of 1.3. Thus, these calculations show that the melanosome separation is very critical with respect to the surface temperature at a melanosome for microsecond pulse durations. For a small absorber distance and microsecond pulse durations, much lower radiant exposures are needed for the same surface temperature when compared with single melanosomes.

Irradiating with multiple pulses, the increase of the background temperature during irradiation, defined as the residual temperature just before the next pulse, has to be considered. This process was modeled with a homogeneously absorbing layer of 5 μm in thickness and 50 μm in diameter, which absorbs 100% of the incoming laser energy. The background temperature was calculated at the center of the disk for a pulsed irradiation (pulse duration, 1 μsec) with a radiant exposure of 200 mJ/cm^2 and a repetition rate of 500 Hz, the result is shown in Figure 10. A temperature increase up to 10°C after 1,000 pulses, which is equivalent to an application time of 2 seconds was calculated. For these laser parameters, the average irradiance is 100 W/cm^2. If this irradiance is continuously applied by a continuous wave laser, the background temperature increases to nearly 20°C after 2 seconds. The radiant exposure for RPE damage at a pulse duration
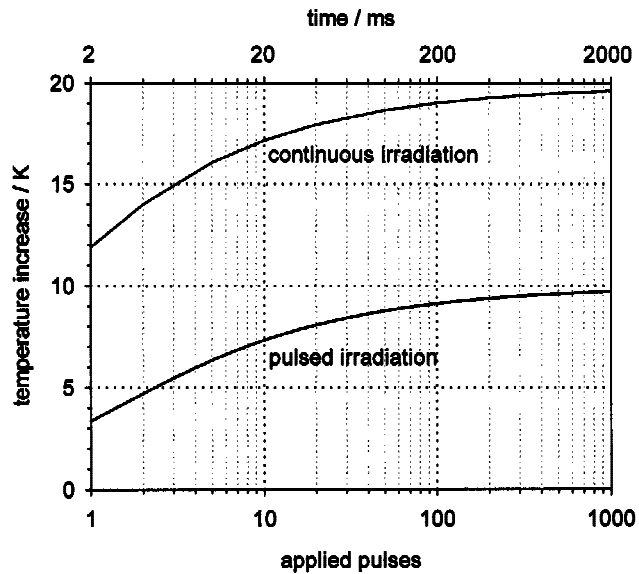
Fig. 10. Calculated increase of the equilibrium temperature increase in the center of a homogeneously absorbing layer 5 μm in thickness with a spot diameter of 50 μm. A radiant exposure of 200 mJ/cm² at a pulse repetition rate of 500 Hz was used, assuming 100% absorption within the layer. The lower line represents the temperature increase before the next pulse, respectively. The upper line shows the temperature increase for a continuous exposure by using 100 W/cm².

of 1 μsec is 95 mJ/cm² for 500 pulses. In this case, a residual temperature of 4.5°C is build up within the RPE at the end of the pulse series.

DISCUSSION

The threshold for microbubble formation around single porcine and bovine melanosomes in suspension and the threshold for RPE cell damage have been investigated. The specimen were irradiated with single and multiple pulses by using pulse durations ranging from the nanoseconds to the microsecond time regimen. Temperature calculations have been performed to analyze the experimental results.

RPE Absorption and Thermal Modeling

Thermal models for the retina, which take a granular structure of the absorption in the melanosomes into account, have already been published by different groups: Heated by melanosomes, which were modeled by cylinders, temperatures in the RPE and neural retina were calculated to understand the selective RPE photocoagulation [1,21]. Thompson et al. used a model with a random distribution of spheres to calculate temperatures around melanosomes [14].

This was used in combination with a second model to calculate the extend of the laser-induced microbubbles around the absorbers to predict the mechanism for retinal damage in the picosecond and nanosecond time regimen [18]. Furthermore, numerical models were established to calculate protein denaturation adjacent to melanosomes [14,21].

The most important parameter in temperature calculations around melanosomes is their absorption coefficient. Measuring the absorption of melanin particles and determining their absorption coefficient is difficult, because of varying properties of different melanins and because of light scattering (Mie-scattering) by the particles, which strongly influences the measurements. By measuring the temperature dependence of the threshold of bubble formation similar to the experiments shown in Figure 5, an absorption coefficients of 180–1,500 cm⁻¹ and 2,400 cm⁻¹ was calculated for melanosomes in skin and from the retina, respectively [22,23]. Nearly 1 order in magnitude higher values in the range of 16,000 cm⁻¹ were calculated from absorption measurements of human retina and RPE layers [7]. Calculations of shock waves around melanosomes only agree with experimental data if an absorption coefficient between 6,000 cm⁻¹ and 8,000 cm⁻¹ was assumed for the melanosomes [24]. These high absorption coefficients are in close agreement to our experimental results (Fig. 5).

Irradiation of Single Melanosomes With Nanosecond Pulses

Vaporization around bovine melanosomes was observed at a threshold radiant exposure of 55 mJ/cm² for 20-nsec pulses at a wavelength of 532 nm. The same threshold radiant exposure was found when using 30-psec laser [10,25]. This result was expected because the thermal relaxation time $\tau_R = r^2/4\kappa$ for a particle of radius r = 0.5 μm yields $\tau_R \approx 420$ nsec, by using the thermal diffusivity of water, $\kappa = 1.5 \times 10^5$ μm²/sec.

The linear dependence of the threshold radiant exposure on the ambient temperature allows one to determine the absorption coefficient and the vaporization temperature of microscopic particles. This method was used for example to determine the absorption of melanosomes in the skin [22,23]. In our experiments, a boiling temperature of 150°C at the surface of bovine melanosomes is calculated by extrapolating the threshold data. This high temperature indicates that local superheating occurs in the fluid layer

surrounding the particles at the onset of bubble growth. Superheating is needed to overcome surface tension when creating a new interface deep in the liquid (homogeneous nucleation) or for bubble growth from a preexisting cavity (heterogeneous nucleation). Bubble growth around a heated particle is most likely a heterogeneous nucleation process, with the particle acting both as a heat source and as a nucleation site. For a bubble to grow from an initial diameter of approximately 1 μm, the vapor pressure must overcome the hydrostatic and the surface pressure, the latter has to be taken into account for particles on the micrometer scale. The pressure P_{sur} associated with the surface tension σ is inversely proportional to the bubble radius r according to $P_{sur} = 2\sigma/r$. With increasing pressure $P = P_{hydro} + P_{sur}$, the boiling temperature of water is elevated. Assuming an initial bubble diameter of 1 μm, an internal pressure of $P = 3.35$ bar can be calculated for $\sigma_{100°C} = 58.9$ mN/m, neglecting its small temperature dependence [26]. The boiling temperature of water at a pressure of 3.35 bar is 137°C. A further increase of the pressure as a consequence of the fast heating does not occur, because heating does not take place under stress confinement conditions, thus, the heating time is much slower than the thermoelastic expansion of water.

The threshold radiant exposure for bubble formation at porcine melanosomes with nanosecond pulses is 1.6 × higher than at bovine melanosomes for nanosecond pulses. When comparing these thresholds, one has to consider size and the absorption coefficient of the different melanosomes, which are of cylindrical shape with the long axis in the order of 1 μm for porcine and 2.5 μm for bovine melanosomes. The reduced threshold of bovine melanosomes may either indicate a slightly higher absorption coefficient or, when assuming similar optical and thermal properties, a lower boiling temperature at the surface due to the smaller surface tension at the larger bovine melanosomes.

With a threshold radiant exposure of 90 mJ/cm^2, a vaporization threshold temperature T_{th} of 150°C (Fig. 5) at the surface of a melanosome can only be calculated for nanosecond exposure by assuming an absorption coefficient around 13,000 cm$^{±1}$ (Fig. 6), by using the thermal properties of water. However, the absorption coefficient μ_a, the heat capacity c_p, and the density ρ of the melanosomes contribute to the threshold temperature and cannot be separated because the threshold radiant exposure F_{th} depends on a ratio of these quantities as shown in equation (1). For melanin, the product of c_p ς is reported to be approximately 20% smaller than that of water [27]. Even if these data will be considered and the absorption coefficient is reduced by 20%, it is still in the regimen of 10^4 cm^{-1}.

Irradiation of Single Melanosomes With Microsecond Pulses

By using the Nd:YLF laser, we found a vaporization threshold radiant exposure that increases with pulse duration. This behavior is expected, because the pulse durations are larger than the thermal relaxation time of single melanosomes; thus, significant heat diffusion takes place during pulse duration. To analyze the experimental data, temperatures were calculated inside and in the surroundings of the irradiated melanosomes.

Calculating the temperature increase for pulses in the microsecond time regimen, the heat conductivity has to be considered. For pressed natural melanin, the thermal diffusivity was found to be close to the water value; thus, deviations can be neglected for temperature calculations [28]. If a vaporization threshold temperature of 150°C is assumed at the surface of a melanosome, the experimental data fit quite well for pulse durations from 250 nsec to 3 μsec when assuming an absorption coefficient of 8,000 cm^{-1} (Fig. 6). However, for an 8-nsec pulse, a radiant exposure of 140 mJ/cm^2 is calculated with this absorption coefficient, which is 55% higher than the experimental value. For the nanosecond pulses, an absorption coefficient as high as 13,000 cm^{-1} has to be assumed to correctly predict the experimental data. The different wavelengths of both systems are not responsible for these differences, because changes of the RPE absorption in this wavelength regimen is below 1% [7].

A possible explanation for this discrepancy might be that the assumption of homogeneously heating the melanosome due to heat diffusion inside the particle is not fulfilled when using very short exposure times. Thus, the surface temperature of the melanosome on the illuminated front side of the particles should be higher than on the back side, and vaporization should first start on the particles front side. If Beer's law of absorption is applied to a spherical particle of 1 μm in diameter with an absorption coefficient of 13,000 cm^{-1}, then the total absorbed energy of the particle is the same as when calculating with a homoge-

neous energy uptake within the whole absorber with a homogeneous absorption coefficient of 8,000 cm^{-1} [14]. Thus, for pulse durations longer than the internal heat dissipation time, a higher radiant exposure to initiate vaporization is expected, because the vaporization temperature has to be reached at the whole surface of the melanosome instead just at the front side. This might explain the strong threshold radiant exposure increase of a factor of two at 250 nsec compared with 8-nsec exposure (Fig. 6).

Mechanisms of Cell Damage

By short-pulsed laser irradiation, RPE cells may either be damaged thermally as it takes place for millisecond irradiation, or by thermomechanical effects causing a disintegration of the cell structure. In the latter case, either pressure or shock waves, emitted due to the fast heating and expansion of the melanosomes, or intracellular microbubble formation around the melanosomes may be responsible for the damage.

Thermal damage of cells is commonly described with the theory of Arrhenius [9], relating the damage to exposure time and temperature. The activation energy and entropy serve as parameters to calculate a damage integral for the damage criteria, which shall be described. Because of the inhomogeneous temperature distribution with high peak temperatures around the melanosomes within the cell, the damage integral strongly depends on the location within the cell, which is taken into account. Birngruber et al. calculated Arrhenius parameters for threshold data on minimal visible retinal damage in the millisecond to second time range [29]. By using these data for our results, the course of the cell damage radiant exposure with pulse duration according to Figure 6 can only be calculated at locations directly at the surface of the absorbers. Even between the melanosomes or at, e.g., the cell membrane, the calculated damage is nearly independent of the pulse durations because heat diffusion significantly reduces the peak temperatures, which dominate the damage integral. The impact of high temperatures at selected locations, such as the surface of the melanosomes, on the cell vitality is unknown; however, we believe that the rapid cell death for single laser pulse exposure as observed here is not caused by a purely thermal mechanism.

The effect of stress waves on biological tissue has been investigated by different groups, a summary is given by Doukas and Flotte [30]. Lin and Kelly found shock waves around melanosomes when irradiating with pulse durations of 30 psec [10,31]. Douki et al. applied stress waves to cultured human RPE cells and found that cell damage is rather related to the stress gradient than to the peak stress. A damage threshold of 70 bar/nsec was determined [12]. However, high peak stress can only occur if the pulse duration τ is in the order or below the acoustic transient time τ_a of the absorber, which is defined as the time, an acoustic wave needs to travel through the absorbing structure. The acoustic transit time for melanosomes is below 1 nsec. Treating the RPE as a homogeneously absorbing layer, the peak stress can be estimated according to the formulas given, e.g., by Sigrist [32]. If the laser pulse duration τ is longer than the acoustic transit time τ_a, $\tau/\tau_a >> 1$, the peak stress decreases proportional to $1/\tau$. According to these formulas, peak compressive stress gradients at the RPE of around 20, 2×10^{-2} and 2.5×10^{-4} bar/nsec were calculated for pulse durations of 8, 250 and 3,000 nsec, respectively, when irradiating the melanosomes with a radiant exposure of 200 mJ/cm^2. The observed cell damage thresholds do not increase with pulse duration, as it should be expected to compensate for the peak pressure decrease according to $1/\tau$ and the pressure gradient proportional to $1/\tau^2$. Thus, cell damage caused by strong pressure or pressure gradients is unlikely. Furthermore, strong pressure transients or RPE cell death have never been observed below the threshold for microbubble formation, even when 30-psec pulse durations are used, which are far below the acoustic transit time of the absorber [31].

With respect to a mechanically induced cell damage, also tensile stress waves have to be considered. They occur by reflections of the compressive wave at boundaries such as the cover slide. Because of the small irradiated spot size of 47 μm, a nearly spherical wave is emitted and reflected at a distance of approximately 1 mm at the cover slide. Thus, its amplitude is significantly lower when it hits the cells again. With respect to its damage potential, Bailey et al. found similar thresholds to kill *Drosophila* larvae with pure positive or pure negative pressure peaks of around 1 μsec in duration [33]. In conclusion, cell damage caused by stress waves cannot be totally excluded, but it is very unlikely in the regimen of pulse durations investigated here, especially for microsecond pulses.

The most probable mechanism of cell damage is the formation of transient microbubbles

arising more or less simultaneously around all melanosomes after the boiling temperature of the intracellular plasma at the surface of the melanosomes is reached. Subsequently, the cell volume significantly increases transiently, which leads to mechanically disruption of cell structures. Lin et al. demonstrated microbubble-induced selective cell killing in pigmented cells [34]. Kelly and Lin showed bubble formation inside bovine RPE cells and found that the threshold radiant exposures for bubble formation and for cell death are similar for single picosecond laser pulses [11].

RPE Cell Damage With Single Pulse Irradiation

For pulse durations of 8 nsec, the vaporization threshold and threshold for cell damage are close. However, the cell damage threshold is significantly lower at pulse durations in the microsecond time regimen. Assuming bubble formation as the primary mechanism to induce cell damage, the lower threshold radiant exposures on RPE cells compared with single melanosomes can be explained by the heat contribution of surrounding melanosomes to the surface temperature of a given melanosome. From the thermal calculation (Fig. 9) it can be seen that the peak surface temperature at a single melanosome increases with decreasing spacing between the absorbers and with higher pulse durations. The experiments show that the RPE damage threshold increases by a factor of 2 when going from 250 nsec to 3 μsec. This factor is also found in temperature calculations when a surface distance of 0.5 μm between the melanosomes is assumed (Fig. 9). In general, a decrease of the threshold radiant exposure for bubble formation in the RPE cell compared with single melanosomes can always be expected, if the ratio of laser pulse duration to the thermal diffusion time $\tau_L/\tau_{diff} > 1$ and the ratio of the spacing between individual melanosomes to the thermal diffusion length $s_{mel}/s_{diff} < 1$.

Transmission electron microscopy (Figs. 1, 3) shows that the distance between the individual melanosomes in human and porcine RPE cells is not regular and varies between almost zero and a few micrometers. Thus microbubble formation will probably take place first at two very close melanosomes when pulse durations are used which allow at least a little thermal diffusion during exposure. In this case, the temperature between the melanosomes is doubled and bubble formation radiant exposures are expected to be reduced up to 50% of the value for single melanosomes. This fact may explain the reduced threshold for RPE damage as shown in Figure 6. In summary, the RPE damage thresholds for single pulse application as observed in the experiments can very well be explained with microbubble formation as the primary origin of cell damage for pulse durations up to 3 μsec.

RPE Cell Damage With Multiple Pulse Irradiation

A decrease of the thresholds for RPE damage is expected when applying multiple pulses. For a variety of pulse durations, pulse numbers, and wavelengths, it is shown that the damage threshold scales with $N^{1/4}$, when N pulses are applied [35]. This empirical functional dependence has been verified by several studies on retinal laser damage thresholds [36,37]. This relation is also used by the ANSI standards for laser safety to describe the reduction of threshold exposure for minimal visible lesions of the eye [35], even for pulse durations at which thermal denaturation is unlikely. At 532 nm and a pulse duration of 5 μsec, Roider et al. observed a reduction of the threshold for angiographic visibility of RPE lesions, which closely fit the $N^{1/4}$ law, when applying a train of up to 500 pulses at a repetition rate of 500 Hz [13]. Griess et al. reported of a cumulative effect for pulse durations of 16 nsec when applying between 1 and 100 pulses with 10 Hz [38]. Bruckner et al. [39] reported a comparable dependence for picoseconds, and Stolarski et al. [40] for 130 femtosecond pulse durations.

The experiments in this study revealed a strong decrease of the threshold radiant exposure up to 500 pulses. However, applying more pulses only a very slightly further decrease is observed. This behavior is not in accordance with the empirical $N^{1/4}$ law. Assuming a thermal damage mechanism, a monotonic decrease of the threshold radiant exposure is expected and can be calculated with the Arrhenius formalism [9]. Because of the unknown activation energy and entropy, predictions are highly uncertain. However, we did not find an appropriate parameter set to describe the decrease of the cell damage over the number of applied pulses with the Arrhenius formalism.

With respect to microbubble formation as the primary mechanism for cell damage, it can be excluded that an increase of the residual temperature before the next pulse reduces the threshold radiant exposure with pulse number: Temperature calculations showed that for a spot diameter of 50 μm, a radiant exposure of 200 mJ/cm² does only result in a temperature increase of approxi-

mately 10°K in the RPE cell (Fig. 10), nearly independent on the number of pulses.

A more reasonable explanation might be the statistical behavior of bubble formation at threshold during the pulse train. A thermomechanical effect as a small increase in cell volume and subsequent minimal cell rupture may to some extend be also cumulative. Small but multiple overstretching of the cell membrane due to microbubbles at only a few sites (e.g., at very close melanosomes) may also cause an irreversible lethal defect. Also for picosecond [38] and femtosecond pulses [40], at which thermomechanics should be responsible for retinal damage, an additivity of multiple exposures was observed.

CONCLUSION

It was shown by fast flash photography that the vaporization threshold radiant exposure around single porcine melanosomes increases almost linearly with pulse duration from 250 nsec up to 3 µsec. Assuming a certain, constant surface temperature of 150°C at the melanosome to be required to initiate bubble formation, calculations of the threshold radiant exposures are in good agreement with the experimental findings when using a melanosome absorption coefficient as high as 13,000 cm^{-1}, which corresponds to a homogeneous absorption coefficient of 8,000 cm^{-1}.

Irradiating RPE cells in an ex vivo retina model with 8-nsec pulse duration, the damage threshold coincides with the threshold for bubble formation at single melanosomes. When increasing the pulse duration, the threshold radiant exposure increases, however, less than for single particles. Assuming bubble formation as the primary mechanism of damage, these findings can be explained by heat diffusion from surrounding melanosomes, which significantly contributes to the surface temperature of an individual granula. Thus, vaporization around the melanosomes and subsequent disruption of the cell structure as the primary damage mechanism can explain the increase of the RPE damage radiant exposure with pulse duration for single pulse exposure.

By using a series of pulses, a further decrease of the damage threshold was observed. However, although thermal coagulation cannot be excluded to be responsible for cell damage, at least for a high number of pulses, it is unlikely because the thresholds for bubble formation at melanosomes are very close to the damage thresholds found for RPE cells. However, in the regimen of microsecond pulse durations, a transition from mechanical to thermal damage is expected [14]. The complexity of the system and uncertainties in optical and thermal parameters do not allow to infer the damage mechanism from the observed damage threshold radiant exposures at different irradiation parameters. Therefore, further studies, which directly observe the mechanisms leading to the cell damage, are needed, e.g., bubble formation during irradiation of vital RPE cells. Furthermore, in vivo studies must be carried out to determine the relationship between the in vitro RPE cell damage and the in vivo RPE defect, which is so far observed by using fluorescein angiography after laser treatment. Independent measurement of the absorption and the thermal properties of melanosomes would be useful to improve the accuracy and reliability of thermal modeling of the retina.

REFERENCES

1. Roider J, Hillenkamp F, Flotte TJ, Birngruber R. Microphotocoagulation: selective effects of repetitive short laser pulses. Proc Natl Acad Sci USA 1993;90:8463–8647.
2. Roider J, Michaud NA, Flotte TJ, Birngruber R. Response of the retinal pigment epithelium to selective photocoagulation. Arch Ophthalmol 1992;110:1786–1792.
3. Roider J, Wirbelauer C, Brinkmann R, Laqua H, Birngruber R. Control and detection of subthreshold effects in the first clinical trial of macular diseases. Inv Ophthalmol Vis Sci 1998;39:104.
4. Roider J, Brinkmann R, Wirbelauer C, Laqua H, Birngruber R. Subthreshold (retinal pigment epithelium) photocoagulation in macular diseases: a pilot study. Br J Ophthalmol 2000;84:40–47.
5. Roider J, Wirbelauer C, Brinkmann R, Laqua H, Birngruber R. Variability of RPE reaction in two cases after selective RPE laser effects in prophylactic treatment of drusen. Graefes Arch Clin Exp Ophthalmol 1999;237:45–50.
6. Roider J, Brinkmann R, Wirbelauer C, Laqua H, Birngruber R. Retinal sparing by selective retinal pigment epithelial photocoagulation. Arch Ophthalmol 1999;117:1028–1034.
7. Gabel VP. Die Lichtabsorption am Augenhintergrund. Habilitation 1974.
8. Gabel VP, Birngruber R, Hillenkamp F. Visible and near infrared light absorption in pigment epithelium and choroid. Congress Series: XXIII Concilium Ophthalmologicum 1978;450:658–662.
9. Birngruber R. Thermal modeling in biological tissue. New York: Plenum Press; 1980.
10. Lin CP, Kelly MW. Cavitation and acoustic emission around laser-heated microparticles. Appl Phys Lett 1998;72:2800–2802.
11. Kelly WM, Lin CP. Microcavitation and cell injury in RPE cells following short-pulsed laser irradiation. Proc SPIE 1997;2975:174–179.

12. Douki T, Lee S, Dorey K, Flotte T, Deutsch T, Doukas AG. Stress-wave-induced injury to retinal pigment epithelium cells in vitro. Las Surg Med 1996;19:249–259.

13. Roider J, El Hifnawi E, Birngruber R. Bubble formation as the primary interaction mechanism in retinal laser exposure with 200-nsec laser pulses. Lasers Surg Med 1998;22:240–248.

14. Thompson CR, Gerstman BS, Jacques SL Rogers ME. Melanin granule model for laser-induced thermal damage in the retina. Bull Math Biol 1996;58:513–553.

15. Brinkmann R, Meyer W, Engelhardt R, Walling JC. Laser induced shockwave lithotripsy by use of an 1 μs Alexandrite laser. Proc SPIE 1990;1200:67–74.

16. Finney DJ. Probit analysis. 3rd ed. London: Cambridge University Press; 1971.

17. Carslaw HS, Jaeger JC. Conduction of heat in solids. 2nd ed. Oxford: Clarendon Press; 1959.

18. Gerstman B, Thompson CR, Jacques SL, Rogers ME. Laser induced bubble formation in the retina. Lasers Surg Med 1996;18:10–21.

19. A Vassiliadis, Ocular damage from laser radiation New York: Plenum Press; 1971.

20. Koechner W. Solid-state laser engineering. 3rd ed. Berlin, Heidelberg, New York: Springer-Verlag; 1992.

21. Pustovalov VK, Khorunzhii IA. Theoretical consideration of the selective thermodenaturation of pigment epithelium layer using short laser pulses. Proc SPIE 1994;2126: 111–115.

22. Jacques SL, McAuliffe DJ. The melanosome: threshold temperature for explosive vaporisation and internal absorption coefficient during pulsed-laser irradiation. Photochem Photobiol 1991;53:769–775.

23. Jacques SL, Glickman RD, Schwartz JA. Internal absorption coefficient and threshold for pulsed laser disruption of melanosomes isolated from retinal pigment epithelium. Proc SPIE 1996;2681:468–477.

24. Strauss M, Amendt P, London RA, Maitland DJ, Glinsky ME, Lin CP, Kelly MW. Computational modeling of stress transient and bubble evolution in short-pulse laser irradiated melanosome particles. Proc SPIE 1997;2975: 261–270.

25. Kelly MW. Intracellular cavitation as a mechanism of short-pulse laser injury to the retinal pigment epithelium. PhD thesis. Boston: Tufts University; 1997.

26. Lide DR. Handbook of chemistry and physics. 76th ed. Boca Raton, New York, London, Tokyo: CRC Press; 1995.

27. Hayes JR, Wolbarsht ML. Modes in pathology: mechanisms of action of laser energy with biological tissues. New York: Plenum Press; 1971.

28. Vitken A, Woolsey J, Wilson BC, Anderson RR. Optical and thermal characterization of natural (sepia officianalis) melanin. Photochem Photobiol 1994;59:455–462.

29. Birngruber R, Hillenkamp F, Gabel VP. Theoretical investigations of laser thermal retinal injury. Health Phys 1985;48:781–796.

30. Doukas AG, Flotte TG. Physical characteristics and biological effects of laser-induced stress waves. Ultrasound Med Biol 1996;22:151–164.

31. Lin CP, Kelly MW. Ultrafast time-resolved imaging of stress transient and cavitation from short-pulsed laser irradiated melanin particles. Proc SPIE 1995;2391:294–299.

32. Sigrist MW. Laser generation of acoustic waves in liquids and gases. J Appl Physiol 1986;60:85–121.

33. Bailey MR, Dalecki D, Child SZ, Raeman CH, Penney DP, Blackstock DT, Carstensen EL. Bioeffects of positive and negative acoustic pressures in vivo. J Acoust Soc Am 1996;100:3941–3946.

34. Lin CP, Kelly MW, Sibayan SAB, Latina MA, Anderson RR. Selective cell killing by microparticle absorption of pulsed laser radiation. IEEE J Select Top Quant Elect 1999;5:963–968.

35. ANSI Standard Z1361. American Standard for the Safe Use of Lasers: American Standards Institute; 1993.

36. Ham WT, Mueller HA, Wolbarsht ML, Sliney DH. Evaluation of retinal exposures from repetitively pulsed and scanning lasers. Health Phys 1988;54:337–344.

37. Stuck BE, Lund DJ, Beatrice ES. Repetitive pulse laser data and permissible exposure limits. Report No 58. San Francisco: Lettermann Army Institute of Research, Presidio of San Francisco; 1978.

38. Griess GA, Blankenstein MF, Williford GG. Ocular damage from multiple-pulse laser exposure. Health Phys 1980;39:921–927.

39. Bruckner AP, Schurr JM, Chang EL. Biological damage threshold induced by ultrashort fundamental, 2nd and 4th harmonic light pulses from a mode-locked Nd:Glass laser. Technical Report 1980; SAM-TR-80-47.

40. Stolarski DJ, Cain CP, Toth CA, Noojin GD, Rockwell BA. Multiple pulse thresholds in live eyes for ultrashort laser pulses in the near-infrared. Proc SPIE 1999;3601: 22–26.